

1 **Meso-scale modelling of aeolian sediment input to coastal dunes**

2

3 Irene Delgado-Fernandez

4

5 Department of Geography, University of Guelph, Guelph, Ontario, Canada

6

7 **Abstract**

8 The collection of a time series coupling hourly wind data (speed and direction)  
9 with sand transport over months has provided new insights into the dynamics of  
10 transport events that input sediment to the foredune at Greenwich Dunes, Prince  
11 Edward Island National Park, Canada. This paper summarises the key aspects of  
12 aeolian sediment movement for a period of 9 months and presents a modelling  
13 approach for resolving aeolian transport to coastal dunes at the meso-scale. The  
14 main hypothesis of the modelling approach is that a small number of key factors  
15 control both the occurrence and the magnitude of transport events. Thresholds  
16 associated with these factors may be used to filter the time series and isolate  
17 potential transport periods over the year. The impacts of nearshore processes  
18 are included in the approach as part of the dynamics of coastal dunes, as are  
19 supply-limiting factors and trade-offs between fetch distances, angle of wind  
20 approach, and beach dimensions. A simple analytical procedure, based on  
21 previously published equations, is carried out to assess the general viability of  
22 the conceptual approach. Results show that the incorporation of moisture and  
23 fetch effects in the calculation of transport for isolated potential transport periods

24 result in improved predictions of sediment input to the dune. Net changes,  
25 measured with three different techniques, suggest that survey data with coarse  
26 temporal resolution underestimates the amount of sand input to the dune,  
27 because sediment is often removed from the embryo dune and foredune by other  
28 processes such as wave scarping. Predictions obtained by the proposed  
29 modelling approach are of the same order of magnitude as measured deposition  
30 and much less than predicted by models based solely on wind speed and  
31 direction. Areas for improvement and alternative modelling approaches, such as  
32 probabilistic approaches similar to weather forecasting, are covered in the  
33 discussion.

34

### 35 **Research Highlights**

- 36 - Aeolian sediment input to coastal dunes is not only a function of wind  
37 speed.
- 38 - This work proposes a modelling approach that improves predictions at the  
39 meso-scale.
- 40 - The incorporation of factors such as fetch and moisture improves  
41 calculations.

42

### 43 **Keywords**

44 Transport events; Beach–dune interaction; Foredune sediment budget; Foredune  
45 evolution

46

47 **1. Introduction**

48

49 Coastal dunes occur at the intersection of two geomorphic systems: the aeolian  
50 realm which is necessary to create them and the suite of nearshore processes  
51 that have a substantial impact on their evolution. A fundamental aspect of  
52 beach–dune interaction is the output of sand from the beach by wind processes,  
53 which represents the primary sediment input to foredunes and is essential in  
54 calculations of coastal dune budgets (Hesp, 1988a, Psuty, 1988a, Psuty,  
55 1988b and Nickling and Davidson-Arnott, 1990). A wind strong enough to  
56 transport sediment is a necessary condition for the creation of coastal dunes  
57 (Sherman and Hotta, 1990) as is the determination of a surface shear stress  
58 threshold value required to set sediment in motion (Coates and Vitek, 1980).  
59 Because of the unique location of coastal dunes within a complex suite of aeolian  
60 and nearshore processes, Delgado-Fernandez and Davidson-Arnott  
61 (2011) suggest that foredune building occurs within a zone whose lower bound is  
62 the minimum wind stress necessary for sand transport and whose upper bound  
63 marks the transition to foredune scarping by waves.

64 Sediment input by wind to the adjacent coastal dune system at the meso-scale is  
65 usually predicted by incorporating hourly wind speed and direction data  
66 measured at standard meteorological stations into sediment transport equations.

67 This procedure often consists of integrating instantaneous transport rate  
68 equations (e.g., Bagnold, 1941, Kadib, 1964, Hsu, 1974 and Lettau and Lettau,  
69 1977) in relation to time and wind direction (e.g., Fryberger and Dean,

70 1979, Kroon and Hoekstra, 1990, Lynch et al., 2008 and Wahid, 2008). The  
71 resulting calculations, however, frequently do not agree with observed values of  
72 sand deposition on the dunes (e.g., Hunter et al., 1983, Sarre, 1989, Chapman,  
73 1990 and Davidson-Arnott and Law, 1996). Supply-limiting factors are often cited  
74 as being responsible for decreasing potential sediment transport rates and thus  
75 confounding predictions of sand input to the foredunes (Nickling and Davidson-  
76 Arnott, 1990). Variables such as moisture, presence of snow cover, fetch  
77 distances, development of gravel lags, surface crusts, and differences in  
78 sediment characteristics may limit sediment supply from the beach surface. All of  
79 these factors can vary rapidly both in space and time and are subject to a strong  
80 seasonal pattern on mid-latitude beaches as a result of storm action, the growth  
81 and decay of vegetation, and temperature fluctuations above and below freezing  
82 (e.g., Ruz and Meur-Ferec, 2004).

83 Research has focused on identifying the effects of each factor individually on  
84 instantaneous transport rates, but there is a lack of understanding of their  
85 combined effect over weeks or months (Bauer and Sherman, 1999). Not all  
86 factors may be of the same relative significance and some may be secondary  
87 when modelling at the meso-scale (e.g., the existence of small surface  
88 irregularities). Previous studies suggest that sediment input to the dune is  
89 primarily controlled by trade-offs between the angle of wind approach, fetch  
90 lengths, event duration and surficial moisture content (Bauer and Davidson-  
91 Arnott, 2003 and Delgado-Fernandez and Davidson-Arnott, 2011), with these  
92 being more or less relevant depending on the type of wind event. Strong

93 alongshore winds, for example, may generate significant amounts of transport,  
94 even with large amounts of superficial moisture content, due to long fetch  
95 distances. However, as a strong wind shifts onshore at some angle, the  
96 probability of generating sediment movement decreases because the combined  
97 effect of surface moisture and short fetch distances can shut down the transport  
98 system (Delgado-Fernandez and Davidson-Arnott, 2011). A strong onshore wind  
99 may even result in wave scarping of the dune instead of aeolian sediment input  
100 from the beach because of storm surge and wave run-up; these, in turn, are  
101 dependent on beach width, wind speed and wind direction. Beach width varies  
102 with beach slope, tidal range, and wave characteristics, whilst wind direction is of  
103 essential importance both in regulating fetch distances and wave run-up  
104 (Nordstrom and Jackson, 1993, Christiansen and Davidson-Arnott, 2004, Bauer  
105 et al., 2009 and Delgado-Fernandez and Davidson-Arnott, 2011).

106 Nearshore processes and foredune scarping (Psuty, 1988a, Psuty,  
107 1988b, Sherman and Bauer, 1993 and Hesp, 2002) and trade-offs between fetch  
108 distances and angle of wind approach (Bauer and Davidson-Arnott, 2003) have  
109 been incorporated into conceptual models of beach and dune interaction, but not  
110 yet into numerical modelling of aeolian sand transport to coastal dunes (Bauer  
111 and Sherman, 1999). There is a need to improve the state of sediment transport  
112 predictions at the meso-scale both by exploring new data sets of wind  
113 characteristics, supply-limiting factors and fetch distances, and by investigating  
114 more comprehensive ways to input data from meteorological stations into  
115 available formulae.

116 This paper makes use of a data base of hourly measurements of winds and sand  
117 deposition over months at Greenwich Dunes to develop a modelling approach for  
118 resolving aeolian transport to coastal dunes on the meso (time)scale. The first  
119 part of the paper introduces the conceptual model (Section 4). This combines  
120 information about the nature of aeolian transport events (Delgado-Fernandez and  
121 Davidson-Arnott, 2011) and elements of the framework described by Bauer and  
122 Davidson-Arnott (2003), which allows parameterization of the fetch and cosine  
123 effects. The essential aspect of the modelling approach is that predictions of the  
124 rate of aeolian sediment transport, based first on wind speed and direction, can  
125 be improved by incorporating relationships between wind, fetch, beach width,  
126 and transport-limiting factors such as moisture content and snow cover. The  
127 second part of the paper evaluates the viability of the approach using a simple  
128 analytical procedure that allows calculation of sand transport from the time series  
129 recorded at Greenwich (5 and 6). Results are compared with actual measured  
130 net deposition at the foredune over the nine month study period and with  
131 predictions based solely on wind speed and direction (Section 7). The discussion  
132 (Section 8) focuses on areas of further research, limitations to obtain appropriate  
133 observations of sediment deposition that can be compared with meso-scale  
134 predictions, and alternative ways (such as probabilistic models) of translating the  
135 conceptual ideas presented here into better predictions of sediment input to  
136 coastal dunes. The purpose of the modelling approach is similar to that of  
137 previous studies such as Fryberger and Dean, 1979 and Davidson-Arnott and  
138 Law, 1990, and it is specifically designed to make use of available data from

139 meteorological stations and/or data that can be measured simply and quickly in  
140 the field since this is the only realistic approach (to date) for predicting sediment  
141 supply to foredunes on a meso-(time)scale basis. Although the choice of a  
142 particular sand transport equation may result in transport rates that differ over an  
143 order of magnitude (Sherman et al., 1998) the focus here lies in the way to apply  
144 available formulae at the meso scale.

145

## 146 **2. Regional setting**

147

148 This research focused on a 1.5 km-long section of a beach–dune system at  
149 Greenwich Dunes, Prince Edward Island (PEI) National Park, Canada (Fig. 1A).  
150 The study area is microtidal and has a relatively narrow beach (30–40 m wide)  
151 consisting predominantly of quartz sand with a mean diameter of 0.26 mm. The  
152 foredune ranges in height from 6 to 10 m and presents a steep stoss slope of  
153 20–25°. The dune crest is aligned from 250 to 270° and the foredune is covered  
154 by marram grass (*Amophila breviligulata*), which exhibits considerable seasonal  
155 variations in height and density. Summer months are usually characterised by  
156 the development of an embryo dune, which is removed or strongly eroded during  
157 winter storms every two or three years.

158 Annual average precipitation is approximately 1000 mm, with peaks from  
159 October to January due to more frequent and intense storms. Snow days (from  
160 November to April) account for 30% of days with precipitation. Ice surrounding  
161 PEI from January to early April forces a continental climate and strongly affects

162 temperatures at Greenwich (which may reach  $-18\text{ }^{\circ}\text{C}$ ). Prevailing winds from the  
163 SW and W (offshore) occur predominantly in summer and are largely unable to  
164 transport sediment to the foredune despite their higher frequency (Walker et al.,  
165 2006). Dominant storm winds from the NE to the NW in the winter can exceed  
166  $100\text{ km h}^{-1}$  on occasions. These have a larger potential to deliver sediment to  
167 the dune but are often associated with storm surges and heavy rain or snow.  
168 Further information of the study site may be found in Walker et al., 2003, Hesp et  
169 al., 2005, Davidson-Arnott et al., 2008, Bauer et al., 2009 and Darke et al., 2009.

170

### 171 **3. Field measurements and data base development**

172

#### 173 3.1. Wind characteristics, fetch distances and supply limiting factors

174 The results presented in this paper cover 9 months of data collection (September  
175 2007–May 2008). The experimental set-up is described in detail in Delgado-  
176 Fernandez et al. (2009) and consisted of a camera system coupled with auxiliary  
177 instrumentation to measure winds and transport processes (Fig. 1B). The camera  
178 system was comprised of three Cannon 8-megapixel digital single lens reflex  
179 (SLR) cameras controlled by a Mumford Time Machine <sup>TM</sup> programmed to take  
180 simultaneous exposures every hour. The cameras were attached to a 6 m-high  
181 mast located on top of the 8 m foredune crest. The set-up was completed with a  
182 2-Dimensional Windsonic anemometer on top of the mast at an elevation of 14 m  
183 above the beach surface. Wind speed and direction were sampled at a frequency  
184 of 1 Hz, with mean values being stored every 2 min on a HOBO Energy Pro data



185 logger. The east-facing camera provided qualitative data on weather and wave  
186 conditions over an area of approximately 1.5 km alongshore. The offshore and  
187 west-facing cameras covered distances of 40 m and 100 m alongshore,  
188 respectively. The images from these two cameras were rectified based on a  
189 model developed using 40–50 ground control points (Fig. 2C), and used to  
190 generate maps of fetch distances, moisture and supply-limiting factors  
191 (Section 3.3).

192

### 193 3.2. Measurements of sand deposition

194 Measuring aeolian sediment transport over weeks to months is a challenging  
195 task. The use of sediment traps at Greenwich was not feasible simply because  
196 traps need to be emptied on a regular basis, including trench traps (e.g., Lynch et  
197 al., 2008). Traps also present a tendency to clog when the sand is wet and it may  
198 be difficult to establish their efficiency (Davidson-Arnott and Law, 1990). Two  
199 Safire saltation probes (Baas, 2004) were deployed at the back beach and  
200 foredune toe (Fig. 2C–D) within the field of view of the cameras. This allowed  
201 assessment of the quality of Safire records by monitoring the height of the  
202 piezoelectric sensor with respect to the sand surface. This height was reset to  
203 5 cm during site visits of every 2 months but the instruments were sometimes  
204 buried or even destroyed and/or removed by nearshore processes (Delgado-  
205 Fernandez and Davidson-Arnott, 2011). Although there were transport events  
206 over which Safires provided good measurements of saltation intensity (e.g., the

207 storm described in Section 7.3) the time series were not continuous and thus not  
208 appropriate for the purpose of long-term analysis.

209 In the absence of other techniques to measure sediment transport rates over  
210 weeks directly (to the knowledge of the author), the approach taken at Greenwich  
211 consisted on using the volume of sediment deposition on the dune as an indirect  
212 measure of sediment transport from the beach. This was based on the work  
213 by Davidson-Arnott and Law, 1990 and Davidson-Arnott and Law, 1996 who  
214 assumed that, if the vegetation is high and dense, windblown sediment from the  
215 beach deposits within a few tens of metres of the vegetation line. Changes in bed  
216 elevation were measured using three techniques with different temporal  
217 resolutions (Fig. 2C–D), with the objective of obtaining a range of values of  
218 measured deposition that, though crude, were adequate to test the validity of the  
219 modelling approach. First, two profiles, located on either side of the camera  
220 tower and spaced 23 m apart, were surveyed using a Differential Global Position  
221 System (DGPS) in May 2007 and June 2008. These provided information on  
222 foredune topography before and after the study period. Second, bedframe posts  
223 spaced approximately 3 m apart were established along each profile from the  
224 embryo dune to the foredune crest, and were surveyed every 2 months. The  
225 bedframe enables measurements that do not interfere with the dynamics of  
226 vegetation and provides data on surface elevation change at 12 points within a  
227 1 m square at each bedframe post (Ollerhead et al., 2003; Fig. 2A). Following the  
228 procedure described by Law (1989) a grid was established so a particular  
229 bedframe post represented a specific area of the dune with an alongshore

230 distance of 23 m per 3 m of shore-normal dune profile (Fig. 2D). The bedframe  
231 technique was designed such that each bedframe lines would encompass the  
232 landward extent of aeolian transport in the vegetated dune (Davidson-Arnott and  
233 Law, 1990 and Davidson-Arnott and Law, 1996). Thus, whilst an individual  
234 bedframe may show wind erosion, there is no loss to the calculation of net  
235 deposition across the profile because deposition is recorded in the landward  
236 stations. It was assumed here that offshore aeolian transport from the embryo  
237 dune was small and could be neglected. Other sources of sediment loss such as  
238 sediment by-passing or wave erosion are discussed in Section 7.3. Finally, a  
239 total of 4 Erosion-Deposition (ED) pins were deployed on the embryo dune and  
240 back-beach. ED pins are permanent rods marked at regular intervals of 2 cm  
241 (Fig. 2B) that are located within the field of view of the cameras. Hourly changes  
242 in surface elevation at each ED pin location could be measured with a precision  
243 of 1 cm by zooming on the RGB images. This permits a much higher temporal  
244 resolution compared to topographic surveys or bedframe measurements.

245

### 246 3.3. Data processing and data base development

247 Detailed information on data processing and geodatabase development may be  
248 found in Delgado-Fernandez and Davidson-Arnott (2011). Measurements of sand  
249 deposition and wind speed and direction were processed using standard  
250 procedures and available software such as Excel and SigmaPlot. The information  
251 from the camera system was processed with ArcGIS 9.2 and PCI Geomatica 9.1,  
252 and followed several steps to extract numerical information such as moisture

253 maps, shoreline position, fetch distances, vegetation density, and ice-snow  
254 cover. Moisture maps were created using calibration curves that transform pixel  
255 brightness into moisture content at the beach surface (Delgado-Fernandez et al.,  
256 2009). The percentage of ice and snow cover was estimated from both the  
257 rectified images and the unrectified images of the east camera, and classified  
258 into 5 classes with increments of 20% which range from 0–20% of snow cover  
259 (first class) to 80–100% of snow cover (last class). Vegetation density raster  
260 datasets were extracted using unsupervised classifications with the Image  
261 Analysis extension from Leica Systems. The shoreline position was digitised in  
262 ArcMap and stored as feature time series, and beach width was obtained from  
263 shoreline position and vegetation extent. Fetch distances were calculated from  
264 beach width and wind direction.

265 Because of the need to integrate spatial and time-series data, a geodatabase  
266 (PEI GDB) was built with ArcCatalog 9.2 to store the information. The PEI GDB  
267 uses four types of time series data: 1) time series tables, which contain time and  
268 value attributes for a given type of observation (e.g., hourly percentage of snow  
269 and ice); 2) attribute series, which store temporal data for a given type of  
270 observation associated with a particular location (e.g., wind speed at 14 m above  
271 the beach recorded by the anemometer); 3) feature series, which represent  
272 sequences of records in which the feature shape varies over time (e.g.; shoreline  
273 position), and; 4) raster series, or time series of raster data in which each raster  
274 is a snapshot in time (e.g., moisture maps). The PEI GDB manages relations  
275 between different factors, permits multiple querying and allows transition

276 between the spatial and the temporal domains using temporal geoprocessing  
277 techniques.

278

## 279 **4. Conceptual model**

280

### 281 4.1. Background

282 A wind event may be simply defined from the point in time when the wind speed  
283 exceeds a threshold value for sand movement to the moment when the wind  
284 decreases to a value below the threshold. Potential transport for any wind event  
285 may be calculated from wind speed and direction using standard equations  
286 (e.g., Hsu, 1974 and Fryberger and Dean, 1979). Analysis carried out  
287 by Delgado-Fernandez and Davidson-Arnott (2011) using a nine month time  
288 series of wind, transport processes and supply-limiting factors at Greenwich  
289 suggested three possible scenarios:

290 1. Wind events may produce no actual transport into the dune for part or all  
291 of the duration of the event because the wind angle may be alongshore or  
292 offshore, or because entrainment of sand from the surface is inhibited by  
293 the presence of snow and ice, short fetch distances, or relatively high  
294 surface moisture content.

295 2. Wind events may produce sand movement to the dunes but the  
296 magnitude of transport is much less than the potential transport predicted  
297 by equations based on wind speed alone because the rate of sand supply  
298 from the surface is reduced as a result of the effects of supply-limiting

299 factors such as moisture, or because the available fetch ( $F$ ) is less than  
300 the critical fetch ( $F_c$ ).

301 3. Transport into the dunes may be of the same order as the potential  
302 transport because there are no supply-limiting conditions (e.g., the  
303 existence of a wide beach, dry sand and winds with an onshore  
304 component).

305

#### 306 4.2. Modelling assumptions

307 The goal of the modelling proposed here is to improve prediction of sediment  
308 input to the foredunes at the meso scale (i.e., over a period of months) by  
309 recognising the role of a few key factors and their synergistic behaviour within a  
310 space that is geometrically constrained. According to Bauer and Sherman  
311 (1999), reductionist studies often follow a procedure that consists on an initial  
312 simplification of transport as a function of wind. The hope is that subsequent  
313 modifications of the equations in order to account for complexities found at a  
314 given surface will produce better explanations of the system behaviour. However,  
315 even if factors such as moisture (for example) are appropriately introduced in  
316 increasingly complex equations, there is no guarantee that these will improve  
317 predictions. A wind well above the threshold of moist sand may produce no  
318 transport as a result of other key aspects that control sediment movement such  
319 as fetch distance or the influence of water levels and wave run-up  
320 (e.g., Nordstrom and Jackson, 1993, Jackson and Nordstrom, 1997, Christiansen

321 and Davidson-Arnott, 2004, Bauer et al., 2009 and Delgado-Fernandez and  
322 Davidson-Arnott, 2011).

323 The main assumption adopted in this study is that sediment transport at the  
324 meso scale could be better predicted based on an initial comprehensive  
325 combination of key parameters. Simplifications may be introduced in the manner  
326 in which this combination is modelled rather than focusing on individual factors.

327 The PEI GDB provides the input data at a level that permits testing of the  
328 modelling approach in some detail, and assessment of the relative improvement  
329 over calculations of potential transport rates based on wind speed alone.

330 Foredune morphological evolution has been a subject of conceptual or  
331 descriptive studies (Hesp, 1988a, Hesp, 1988b, Psuty, 1988a, Sherman and  
332 Bauer, 1993 and Hesp, 2002) but it is difficult to model numerically and is beyond  
333 the scope of this study. The focus here lies on the prediction of sediment input to  
334 the foredune which, combined with sediment output, will dictate whether the dune  
335 will grow or erode (Psuty, 1988b). The area a few metres in front of the foredune  
336 is particularly complex in terms of the wind flow and is often characterised by flow  
337 steering and stagnation (Hesp et al., 2005 and Walker et al., 2006). When an  
338 embryo dune is present in this zone, the embryo dune vegetation retards  
339 sediment transport, and there is a complex relationship between the sand  
340 accumulated within this vegetation and the sand that is actually transported to  
341 and up the dune slope. Much of the sand deposited within the embryo dune may  
342 never reach the dune slope because of erosion by waves (e.g., Christiansen and  
343 Davidson-Arnott, 2004). The model presented here calculates sediment output

344 from the beach and predicts the mass of sand crossing the “blue line” in Fig. 3A–  
345 B. This study does not deal with how sediment is distributed over the dune or  
346 with the resulting dune morphologies, which are affected by processes not  
347 considered here (e.g., interaction of wind and topography, wave scarping,  
348 vegetation patterns). Fig. 3B shows a schematic representation of a beach–dune  
349 system, and includes the output area in front of the embryo dune as explained  
350 above. According to Bauer and Davidson-Arnott (2003) sediment transport rates  
351 may be predicted using Bagnold-type equations when the available fetch ( $F$ ) is  
352 equal to or larger than the critical fetch ( $F_c$ ) but calculations should account for  
353 the reduction in transport due to the fetch effect when  $F < F_c$  (see Section 6.2).  
354 The red band on the beach surface (Fig. 3B) indicates the distance at which  
355 transport is fully developed for a given wind speed ( $F = F_c$ ) and thus separates  
356 the zone where the fetch effect should be considered from that where it does not  
357 apply.

358

#### 359 4.3. Modelling approach

360 The modelling approach consists of two steps (Fig. 4): 1) filtering of the time  
361 series; and 2) calculation of transport for individual events.

362

##### 363 4.3.1. Filtering

364 Filtering removes periods when transport toward the dune cannot occur because  
365 wind speed is below the threshold for dry sand or wind direction is offshore. It  
366 also removes those times when the magnitude of supply limiting factors such as



367 moisture, snow and ice, and fetch length exceed a threshold above which there  
368 is no potential for sand entrainment by the wind. In doing so, the filtering isolates  
369 potential transport periods (PTPs) and provides information on the frequency and  
370 duration of such events.

371

#### 372 4.3.2. Calculation of transport for individual PTPs

373 The filtering simplifies the time series and reduces the volume of information to  
374 analyse. This allows concentrating on the details of particular PTPs, such as the  
375 spatial pattern of factors at an hourly scale (e.g., maps of moisture content).

376 PTPs may be characterised by different levels of complexity depending on the  
377 dynamics of a few key controlling variables, namely wind speed and direction,  
378 fetch distance (and thus beach width), and superficial moisture content. This  
379 paper proposes the following classification of PTPs:

380

381 Type A: dry conditions—no restriction

382 PTPs may occur during onshore or oblique winds blowing over a relatively wide  
383 beach with a dry surface (Fig. 5A). The saltation system is allowed to develop  
384 fully for the incoming wind speed (fetch is not important) and thus transport may  
385 be calculated at the output area using Bagnold-type equations and modified by  
386 the cosine of wind angle following the procedure suggested by Bauer and  
387 Davidson-Arnott (2003). On narrow beaches this type of event will only occur  
388 under low wind speeds (short critical fetches). For wide beaches the range of  
389 wind speeds involved in Type A transport will likely increase.

390

391 Type B: dry conditions — restricted

392 PTPs may consist of medium complexity transport periods resulting from  
393 changes in the position of the area where  $F = F_c$  due to varying wind speeds  
394 and/or direction. Bagnold-type equations may be applied at an hourly basis  
395 when  $F \geq F_c$ , whilst transport is reduced due to the fetch effect when  $F < F_c$  (i.e.,  
396 when the red band is landward of the output area in Fig. 5B). This type of PTP  
397 may follow two general patterns:

398 B1 - Time-varying wind speed restrictions; wind direction (and thus fetch  
399 length,  $F$ ) may be relatively steady, but wind speed fluctuates so that there are  
400 periods of time where  $F < F_c$  ( $t_2$ ).

401 B2 - Time-varying, wind direction restrictions; changes in wind direction over  
402 strong wind events may introduce complexities associated with available fetch  
403 distances. On a narrow beach a strong wind may only fully develop saltation with  
404 highly oblique wind angles ( $t_1$ – $t_3$ ) with transport being limited when the wind  
405 direction is close to shore perpendicular because  $F < F_c$  ( $t_2$ ).

406

407 Type C: moist conditions

408 Transport often develops under very complex conditions with changes in wind  
409 speed, direction, fetch lengths and moisture. The saltating system during Type C  
410 PTPs is rarely fully developed because moisture limits entrainment and interacts  
411 with the fetch effect in ways that are still not fully understood (Delgado-  
412 Fernandez, 2010). Davidson-Arnott et al. (2008) suggest that the curve relating

413 transport rate with fetch distance over a moist surface may be similar to that over  
414 a dry surface, only with a longer critical fetch “adjusted” to wet conditions. In  
415 other words, it is likely that the proportion of time during which the red band  
416 in Fig. 5C is landward from the output area will increase, thus reducing transport  
417 rates at the top of the beach. PTPs Type C may be divided into two general  
418 categories:

419 C1 - Uniform moisture restrictions: moisture content is included via an increase of  
420 the calculated  $F_c$  for an incident wind speed (Section 6.2). Moisture interacts in  
421 complex ways both with the sediment transport threshold and the mass flux on  
422 beach surfaces. The maximum sediment flux for dry sand as predicted by  
423 transport equations (e.g., Bagnold, 1941 and Hsu, 1974) may be lower than that  
424 for moist sand, similar or even higher if sediment moves across a moist, harder  
425 surface ( McKenna Neuman and Maljaars Scott, 1998 and Davidson-Arnott et al.,  
426 2008). However, there seems to be enough evidence suggesting that the critical  
427 fetch increases with increasing beach surface moisture (Delgado-Fernandez,  
428 2010).

429 C2 - Spatially complex moisture restrictions (“patch”): areas with large amounts  
430 of moisture content may be considered sinks rather than source zones. The fetch  
431 length can be thus measured as the distance between moisture patches and the  
432 output area, that is, moisture zones reduce the actual space for transport to  
433 develop. The data set obtained at Greenwich contains several onshore transport  
434 periods where the foreshore area became progressively wetter as a thin layer of  
435 sediment was removed by wind gusts whilst the back-beach became

436 progressively drier because of accumulation of dry sand. This resulted in a  
437 decrease of the fetch distance over time. The approach taken here oversimplifies  
438 the dynamics of events of type C2 but incorporates hourly variations of fetch  
439 distances.

440

## 441 **5. Description of the data set**

442

443 The input data for the model consisted of hourly values of wind speed and  
444 direction (obtained from 2 min records from the Windsonic on top of the  
445 mast; Section 3.1), beach width, snow and ice cover, fetch distances and  
446 moisture content. The PEI GDB contains detailed information on the spatial  
447 distribution of some of these factors for every given image (e.g., shoreline  
448 position) (Section 3.1) but for the purpose of this paper only hourly averages  
449 were considered.

450 Moisture maps were stored at a 0.05 m grid resolution within the PEI GDB. The  
451 mean hourly value was obtained by considering an area of 10 m in front of the  
452 embryo dune. This area was usually out of the tidal influence and wide enough to  
453 obtain representative mean values of moisture content due to rain fall, snow melt,  
454 or large wave swash. The mean value for moisture ( $\mu$ ) was then classified into  
455 three categories: 1) “dry”:  $\mu \leq 2\%$ ; 2) “medium”:  $2\% < \mu < 10\%$ ; and; 3) “wet”:  
456  $\mu \geq 10\%$ . The objective of this classification was to broadly differentiate periods of  
457 time when moisture is not likely to play a major role (“dry”) from moments when  
458 moisture completely prevents transport (“wet”) (Davidson-Arnott et al., 2008).

459 The “medium” class comprises all cases (the majority) when complex interactions  
460 between wind thresholds and rapid drying of superficial sediments are expected  
461 (Wiggs et al., 2004 and Davidson-Arnott and Bauer, 2009).

462 Snow-ice cover was averaged from measurements obtained from three  
463 simultaneous images taken from the cameras. Delgado-Fernandez and  
464 Davidson-Arnott (2011) observed that transport was completely shut down at  
465 Greenwich when half or more of the beach was covered by ice-snow.

466 Complications associated with modelling aeolian sand transport in the presence  
467 of snow are beyond the scope of this paper and thus only the threshold  
468 associated with ice-snow presence is used here in the filtering stage  
469 (Section 6.1). Beach width was obtained from mean values of shoreline position  
470 and vegetation extent for the offshore and west-facing cameras. The available  
471 fetch distance (F) was then calculated considering the relation between beach  
472 width (W) and the angle of wind approach from shore perpendicular ( $\alpha$ ) using the  
473 following expression:

474

$$F = W / \cos\alpha \quad \text{Equation(1)}$$

475

476 Finally, the majority of night exposures were enhanced as described by Delgado-  
477 Fernandez et al. (2009) which allowed extraction of the variables mentioned  
478 above. There were only a few very dark night shots when measurements were  
479 not possible and thus mean values were interpolated based on conditions during  
480 the last exposure in the evening and the first exposure the following morning and

481 on predicted tidal elevation. This introduced a small level of uncertainty but  
482 resulted in a data set of synchronised mean hourly values of wind speed and  
483 direction, snow-ice cover, beach width, fetch distances, and moisture content that  
484 could be used for modelling purposes.

485

## 486 **6. Analytical procedure**

487

488 Section 8 discusses possible alternatives to develop numerical models based on  
489 the approach described in Section 4. Only a simple analytical procedure was  
490 conducted here to test whether calculations of sediment input to coastal dunes  
491 based on deterministic formulae (e.g., Hsu, 1974, Fryberger and Dean,  
492 1979 and Davidson-Arnott and Law, 1996) may be improved using the modelling  
493 approach.

494

### 495 **6.1. Filtering the time series**

496 The numerical values for the thresholds used for isolating PTPs were based on  
497 the work of Delgado-Fernandez and Davidson-Arnott (2011). These authors  
498 observed that no significant sediment input to the dunes occurred at Greenwich  
499 under any of the following conditions: wind speed ( $U$ )  $< 6 \text{ m s}^{-1}$ ; offshore wind  
500 direction; “wet” surfaces ( $\mu \geq 10\%$ ); snow and ice cover  $> 50\%$ ; and beach  
501 inundation by nearshore processes. This is the combination of all thresholds is a  
502 necessary condition for the potential existence of transport:

503

$$\begin{array}{c}
 U > 6 \text{ m s}^{-1} \\
 \text{onshore component} \\
 \text{if } \rightarrow \quad \mu < 10\% \quad \rightarrow \text{PTP} \\
 W > 0 \text{ m} \\
 \text{snow and ice} < 50\%
 \end{array}$$

504

505 Whilst any one of these thresholds will inhibit transport, the PTPs isolated by this  
 506 procedure may not all include periods of actual transport (Section 8). The filtering  
 507 technique, however, narrows down potential transport events whilst preventing  
 508 the loss of data. Importantly, and because of the inclusion of beach width (and  
 509 therefore fetch distance) as a necessary condition for transport to develop, the  
 510 filtering eliminates from the time series those periods where storms with strong  
 511 onshore winds produce storm surge and wave run up that inundates the beach.

512

### 513 6.2. Calculating transport for individual PTPs

514 A key aspect of the conceptual model is the importance of considering other  
 515 factors in addition to wind speed and direction. The choice of a particular formula  
 516 for predicting sediment transport is important for calculating absolute values of  
 517 sediment output from the beach, but establishing the suitability of a particular  
 518 equation over another is beyond the scope of this paper. For detailed reviews  
 519 about instantaneous transport equations see Horikawa et al., 1986, Nickling,  
 520 1994 and Sherman et al., 1998. The focus here was to assess the performance  
 521 of the two modelling steps and for this purpose any relatively simple expression  
 522 relating wind speed and sediment transport rate was sufficient. The empirical  
 523 equation proposed by Hsu (1974) was selected here simply because it relates

524 transport directly with wind velocity rather than with shear velocity. Estimations of  
525 shear velocity require measurements of velocity profiles or detailed knowledge of  
526 the roughness length ( $z_0$ ) and internal boundary layer development, which  
527 changes considerably spatially and temporally (Davidson-Arnott and Law, 1996).  
528 Whilst it would have been possible to estimate shear stress from assumptions of  
529 surface roughness this was likely to be a constant in this study and therefore  
530 would have had no impact to improve the modelling. Hsu's formula introduces a  
531 degree of uncertainty because Hsu adjusted the constant to the particular  
532 beaches he worked on. However, it is based on a previous version using shear  
533 velocity (Hsu, 1973) which predicts sediment transport rates close to those  
534 calculated by Bagnold's (1941) model and that are in the middle range compared  
535 to a number of models tested by Sherman et al. (1998). Hsu's equation was also  
536 adopted in a similar type of study by Davidson-Arnott and Law (1996), who  
537 included the cosine effect for its use when wind speed and direction are the only  
538 data available. According to these authors, the potential transport rate into the  
539 dunes per unit alongshore distance ( $q_n$ ,  $\text{kg m}^{-1} \text{s}^{-1}$ ) may be expressed as:

540

$$541 \quad q_n = 1.16 \times 10^{-5} \times U^3 \cos \alpha \quad \text{equation (2)}$$

542

543 where  $U$  is hourly wind speed in  $\text{m s}^{-1}$ . Thus  $q_n$  is the predicted rate of sediment  
544 movement at the output area (Fig. 5A) based on wind speed and direction alone,  
545 and hence only applicable in type A PTPs (no restrictions), or during  $t_1$  and  $t_3$  in  
546 type B PTPs.



547 Despite advances in the modelling of the fetch effect in agricultural areas  
548 (e.g., Stout, 1990, Gillette et al., 1996 and Fryrear et al., 2000) there is no  
549 accepted equation describing the increase of sediment transport rate with fetch  
550 distance on beaches (Delgado-Fernandez, 2010). This poses major difficulties  
551 when trying to incorporate the fetch effect into the modelling of aeolian sediment  
552 input to the foredunes, especially with strong winds associated with long critical  
553 fetch distances (Davidson-Arnott and Law, 1990, Spies and McEwan,  
554 2000 and Dong et al., 2004) (during t2 in PTPs type B). Bauer and Davidson-  
555 Arnott (2003) proposed four harmonic functions to describe the increase of  
556 sediment transport with distance. According to Delgado-Fernandez (2010), their  
557 Equation 2a is consistent with other empirical equations in agricultural areas and  
558 thus it is used in here:  
559

$$q_n(F) = q_n \sin\left(\frac{\pi}{2} \frac{F}{F_c}\right) \quad \text{Equation (3)}$$

560  
561 Eq. (3) needs numerical values for  $F_c$  but there are no current methods to  
562 calculate this (Delgado-Fernandez, 2010). There is, however, some supporting  
563 evidence suggesting that it is reasonable to estimate  $F_c$  given a particular wind  
564 speed blowing over a dry surface. Fig. 6 shows a high correlation between wind  
565 speed and the distance where transport attains a maximum as reported in the  
566 numerical simulations by Spies and McEwan (2000) (curve A) and field results  
567 by Davidson-Arnott and Law (1990) (curve B). Curve B has a steeper slope in

568 agreement with other studies in natural areas showing critical fetch distances that  
569 are longer than those found by numerical simulations or laboratory analysis  
570 (e.g., Gillette et al., 1996, Fryrear et al., 2000 and Davidson-Arnott et al., 2008).

571 The expression associated with curve B is used here:

572

$$573 F_c = 4.38 \times U - 8.23 \quad \text{Equation (4)}$$

574

575 This permits the generation of a set of  $F_c$  for a relevant range of wind speeds ( $U$ )  
576 and testing of the modelling approach. No claim is made here regarding the  
577 general applicability of Eq. (4) beyond this analytical procedure.

578 Whilst the filtering deals with “wet” periods and Eqs. (2) and (3) are used for “dry”  
579 PTPs type A and B (respectively) there is a need to include “medium”  
580 ( $2\% > \mu > 10\%$ ) moisture content values characteristic of PTPs type C. There are  
581 several equations relating the threshold of sand movement with moisture content  
582 (e.g., Belly, 1964, Logie, 1982 and McKenna Neuman and Nickling, 1989) or with  
583 sediment transport rates (e.g., Hotta et al., 1984 and Sarre, 1987) but none on the  
584 relation between moisture and critical fetch distances (Delgado-Fernandez,  
585 2010). Ideally this research would benefit from studies targeting aeolian sediment  
586 transport during PTPs Type C, the most common situation at the meso scale  
587 (Delgado-Fernandez and Davidson-Arnott, 2011). In the absence of tools to  
588 model the complex interactions between moisture, fetch, and wind  
589 characteristics, the following procedure was adopted. 1) Based on observations  
590 by Davidson-Arnott et al. (2008) it was assumed that homogenous moisture

591 content (PTPs Type C1) increased the critical fetch calculated for dry sand ( $F_c$ )  
 592 to a new larger value ( $F_{c\mu}$ ) for a given wind speed with the increase being  
 593 proportional to the value for moisture content. On this basis, a simple arbitrary  
 594 scheme was utilised, with  $F_{c\mu}$  resulting from an increase of  $F_c$  by 50% when  
 595  $4\% \leq \mu < 6\%$ , and by 75% when  $6\% \leq \mu < 10\%$ . For  $2\% \leq \mu < 4\%$  it was assumed  
 596 that the surface was likely subject to rapid drying and stripping of sand grains by  
 597 wind gusts (Wiggs et al., 2004) and  $F_c$  was not modified. 2) When clear  
 598 “patches” of moisture vs. dry zones were present at the beach surface,  $F_c$  was  
 599 calculated for dry sand but the available fetch ( $F$ ) was measured from the  
 600 landward limit of damp areas. Again, it is acknowledged here that this is an over-  
 601 simplified procedure adopted to permit operationalization of the model in the  
 602 absence of an adequate technique based on field and/or laboratory data.  
 603 Fig. 7 shows a diagram of the analytical procedure. The steps may be  
 604 programmed with any scripting language such as Python or even conducted with  
 605 Excel. For a given hour in a selected PTP the model calculates  $F_c$  based on wind  
 606 speed using Eq. (4), checks the mean moisture content, and obtains (if  
 607 applicable)  $F_{c\mu}$ . If  $F_c$  (or  $F_{c\mu}$ )  $\leq F$  (red band in Fig. 5 is seaward from the output  
 608 area) then the model applies Eq. (2). If  $F_c$  (or  $F_{c\mu}$ )  $> F$  the model applies Eq. (3).  
 609 Finally, the procedure calculates the total amount of transport for a particular  
 610 PTP (QPTP) by adding hourly values of sand transport rates:

611

$$Q_{PTP} = \sum_{q=1}^{q=n} q_n \quad \text{Equation (5)}$$

612

## 613 **7. Modelling approach results and testing**

614

615 The modelling approach predicts a total amount of sand crossing the output area  
616 over any period of time longer than 1 h. To compare this amount with actual  
617 deposition at the dune the assumption is that the embryo dune and foredune trap  
618 everything that is delivered to them over the time period considered. There are  
619 several uncertainties associated with this. First, survey methods or bedframe  
620 posts record net deposition, and thus do not reflect potential periods of erosion.  
621 Second, sediment by-passing and being transported over the dune crest and  
622 beyond is not measured by the techniques used in this study. These limitations  
623 are discussed in the following sections.

624

### 625 7.1. Measured deposition over 9 months

626 Fig. 8 shows the results of both topographic profiles (A) and bedframe  
627 measurements (B). Net changes from May 2007 to June 2008 were minimal and  
628 concentrated at the lower sections of the foredune (lower slope and dune toe)  
629 and embryo dune. Bedframe posts landward of the foredune crest (1–3 W)  
630 showed no substantial changes over the study period. The largest net deposition  
631 occurred from October to December 2007, which was probably related to a single  
632 very strong transport event on November 9–13 (Section 7.3). Table 1 shows  
633 values of erosion and deposition recorded by each of the bedframe posts (BP).  
634 The mean net change over the dune stoss slope (bedframe posts seaward from

635 the crest, cross-shore distance = 18 m) was 9.2 cm on Line E and 6.9 cm on line  
 636 W, which give an average accretion of 8.05 cm over 9 months.

637

638 Table 1. Results for bedframe posts (BP) over 9 months of data collection. Note  
 639 that BP1-3 in line W was not included in the calculations. Changes are expressed  
 640 in cm. Fig. 2 and Fig. 8 show the location of the bedframe posts.

Line E	Deposition	Erosion	Net change	Location	Net change	Erosion	Deposition	Line W
–				Dune trough	– 1.94	– 2.41	0.47	BP1
–				Dune trough	1.79	– 0.33	2.12	BP2
–				Dune trough	0.43	– 1.45	1.88	BP3
BP1	1.48	– 0.47	1.01	Dune crest	– 0.94	– 1	0.06	BP4
BP2	3.9	– 2.64	1.26	Upper slope	1.81	– 0.28	2.09	BP5
BP3	6.5	– 0.47	6.03	Upper slope				–
BP4	20.47	– 2.83	17.64	Low stoss slope				–
BP5	20.52	– 0.28	20.24	Dune toe	13	– 4	17	BP6
–				Embryo dune	13.95	– 0.36	14.31	BP7
	10.6	– 1.3	9.2	Mean	6.9	– 1.4	8.4	

641

642 Davidson-Arnott and Law (1996) used the following relationship to convert values  
 643 of volume of sediment deposition (or erosion) to a total sediment transport (q):

644

$$\frac{dq}{dx} = \left( \frac{dh}{dt} \right) \gamma \quad \text{Equation (6)}$$

645

646 where  $dh/dt$  is the change in elevation over a particular time period and  $x =$   
647 distance along profile. A mean value for bulk density ( $\gamma$ ) of  $2082 \text{ kg m}^{-3}$  was  
648 obtained from sand samples at the laboratory and corresponded to that  
649 estimated assuming a sediment density of  $2650 \text{ kg m}^{-3}$  (Bagnold, 1941) and a  
650 porosity of 0.23 (Fetter, 1994). Note that for the reason noted above, the  
651 bedframes landward of the dune crest (1–3 W) were not considered in the  
652 calculations. The net average change over 9 months recorded by the bedframes  
653 was  $Q_{\text{BF-net}} = 3017 \text{ kg m}^{-1}$  ( $1.45 \text{ m}^3 \text{ m}^{-1}$ ), based on a net average accretion of  
654 8.05 cm along the profile.

655 The values in Table 1 reflect net quantities, and thus may be missing important  
656 information about sediment deposition or erosion between surveys. In fact the  
657 bedframe posts recorded a few periods of erosion (or possible compaction),  
658 which introduces the question of whether net changes over months  
659 underestimate sand delivered by wind over shorter periods of time. If only  
660 deposition is considered (average = 9.5 cm) the gross amount of sand deposited  
661 over the dune is increased to  $Q_{\text{BF-only\_dep}} = 3560 \text{ kg m}^{-1}$  ( $1.71 \text{ m}^3 \text{ m}^{-1}$ ).

662 Fig. 9 displays the ED pins hourly records during the 9 months of study period.

663 Elevation changes were quite dynamic at the back beach and embryo dune, with  
664 many small erosion and deposition periods of less than  $\pm 5$  cm, and several of  
665 more than  $\pm 10$  cm. Table 2 shows the result of summing periods of erosion and

666 deposition, and the net changes recorded at the end of the study period by the  
 667 ED pins. The average net deposition at the embryo dune was 26.5 cm. This  
 668 results in  $Q_{ED-net} = 4966 \text{ kg m}^{-1} (2.38 \text{ m}^3 \text{ m}^{-1})$  according to Eq. (6). The average  
 669 gross deposition (erosion not considered) at the embryo dune was approximately  
 670 83 cm, which equates to  $Q_{ED-only\_dep} = 15552.5 \text{ kg m}^{-1} (7.47 \text{ m}^3 \text{ m}^{-1})$ . A  
 671 discussion about the significance of these differences is presented in Section 8.  
 672  
 673 Table 2. Results for ED pins over 9 months of data collection. Changes are  
 674 expressed in cm. Fig. 2 shows the location of ED pins.

ED pin	Deposition	Erosion	Net change	Location
1	94	- 67	27	Embryo dune
2	72	- 46	26	Embryo dune
3	51	- 60	- 9	Back beach
4	71	- 67	4	Back beach
Mean ED1-2	83	- 56.5	26.5	Embryo dune
Mean ED3-4	61	- 63.5	- 5	Back beach

675

## 676 7.2. Sediment input predicted over 9 months

677 The analytical procedure was run using data for a nine month period  
 678 (6576 h). Table 3 summarises the output of both the filtering ( $Q_{filtering}$ ) and  
 679 calculation of transport over isolated PTPs ( $Q_{PTP}$ ).  $Q_n$  is the total amount of  
 680 sediment transport predicted using Eq. (2), which represents the quantity that  
 681 would be calculated using a traditional approach based solely on wind speed and  
 682 direction (e.g., Fryberger and Dean, 1979 and Wahid, 2008).  $Q_{PTP}$  represents the  
 683 actual output of the analytical procedure, or transport calculated for all PTPs  
 684 considering supply-limiting conditions and different types of events. Results are

685 expressed in  $\text{kg m}^{-1}$  ( $Q_i$ ), the number of hours of predicted transport and the  
 686 percent of time they represent over 9 months, and, most importantly, the relation  
 687 with measured values ( $Q_i$  respect  $Q_{\text{BF-net}}$ ). For consistency with previous studies  
 688 (e.g., Davidson-Arnott and Law, 1996) the modelling output was compared  
 689 against the average net change recorded by the bedframes over the entire  
 690 foredune (BP 1–3 W excluded). The rest of observed changes have been  
 691 included in Table 3 for discussion purposes (Section 8).

692

693 Table 3. Output of the modelling procedure and comparison of predicted  
 694 quantities with observed net deposition at the embryo dune and foredune.  $Q_n$ :  
 695 total amount of sediment transport predicted using Eq. (2);  $Q_{\text{filtering}}$ : output of the  
 696 filtering step;  $Q_{\text{PTP}}$ : output of the calculation of transport over isolated PTPs;  $Q_{\text{ED-}}$   
 697  $_{\text{only\_dep}}$ : average gross deposition (erosion not considered) measured by ED pins  
 698 at the embryo dune;  $Q_{\text{ED-net}}$ : average net change measured by ED pins at the  
 699 embryo dune;  $Q_{\text{BF-only\_dep}}$ : average gross deposition (erosion not considered)  
 700 measured by bedframes over the foredune;  $Q_{\text{BF-net}}$ : net average change  
 701 measured by bedframes over the foredune. Note that in the particular case of this  
 702 time series the majority of events resulting in wave run-up or storm surge (beach  
 703 width  $> 0$  m) were already filtered by the effects of high amounts of moisture  
 704 content or snow-ice cover (thus the low values associated to a few remaining  
 705 periods of time).

Factor		No. of hours	% time	$Q_i$ ( $\text{kg m}^{-1}$ )	$Q_i$ respect $Q_{\text{BF-net}}$
Predicted Q					
$Q_n$	Wind	2018	31	86 458	28.7 $Q_{\text{BF-}}$



	Factor	No. of hours	% time	$Q_i$ ( $\text{kg m}^{-1}$ )	$Q_i$ respect $Q_{\text{BF-net}}$
	speed $> 6 \text{ m s}^{-1}$ onshore direction				net
$Q_{\text{filtering}}$	Snow $< 50\%$ cover	1442	22	55 073	18.2 $Q_{\text{BF-net}}$
	Moisture $< 10\%$	1119	17	35 921	11.9 $Q_{\text{BF-net}}$
	Beach width <sup>1</sup> $> 0 \text{ m}$	1110	16.9	35 632	11.8 $Q_{\text{BF-net}}$
$Q_{\text{PTP}}$	Fetch effect	1110	16.9	24 877	8.2 $Q_{\text{BF-net}}$
	Moisture	1110	16.9	18 663	6.2 $Q_{\text{BF-net}}$
Observed $Q$					
$Q_{\text{ED-only\_dep}}$	–	–	–	15 552	5.1 $Q_{\text{BF-net}}$
$Q_{\text{ED-net}}$	–	–	–	4966	1.6 $Q_{\text{BF-net}}$
$Q_{\text{BF-only\_dep}}$	–	–	–	3560	1.2 $Q_{\text{BF-net}}$
$Q_{\text{BF-net}}$	–	–	–	3017	1

706

707 Predicted sediment output from the beach based only on wind speed and  
708 direction ( $Q_n$ ) was almost 29 times larger than observed net deposition at the  
709 foredune measured by the bedframes ( $Q_{\text{BF-net}}$ ). The filtering improved the  
710 accuracy of transport predictions by decreasing the calculated value to a quantity  
711 11.8 times larger than the observed net deposition. Finally, the effects of  
712 moisture and the fetch effect introduced to calculate transport for each PTP  
713 resulted in predicted quantities that were 6.2 times larger than the observed  
714 deposition.

715

716 7.3. Measured deposition over a storm event

717 A storm that began on November 9, 2007, was selected as an example of the  
718 performance of the modelling approach over a particular wind event because of  
719 several tradeoffs between key factors, such as the cosine and the fetch effect, or  
720 the influence of moisture content. This event is described in detail by Delgado-  
721 Fernandez and Davidson-Arnott (2011), and is a typical example of transport  
722 occurring under Type C conditions (Section 4.3.2).

723 Fig. 10 displays the time series of wind speed and direction (A), tidal elevation  
724 and saltation intensity recorded by a Safire located at the back-beach (B), beach  
725 width (C), and fetch distances and classified moisture content (D) (Section 5).

726 The wind started blowing over the threshold for dry sand movement at 10 am on  
727 November 9 and died out at 3 am on November 13, resulting in a wind event  
728 duration of 90 h. Strong transport was observed under specific conditions on  
729 November 11. Relatively low wind speeds combined with moisture content from 2  
730 to 4% precluded grain entrainment on November 9. An increase in wind speed  
731 on the morning of November 10 generated limited sand transport, which fully  
732 developed during the day due to a further increase in wind speed coinciding with  
733 low tide and oblique angle of wind approach. A gradual change in wind direction  
734 to onshore-perpendicular decreased the available fetch distance and produced  
735 wave up-rush eventually resulting in the beach inundation. The peak wind  
736 speeds coincided with onshore winds thus precluding sediment movement during  
737 the rest of the event because of storm surge and wave run-up.

738 The complexity of the ED pin records at the end of the storm illustrates some of  
739 the points raised in the discussion (Section 8). ED pins 1 and 2 recorded net  
740 deposition of 4 and 25 cm respectively at the embryo dune (see Fig. 2 for  
741 location). ED 4 recorded 10 cm of net deposition at the back beach but ED 3  
742 recorded 15 cm of erosion at the back beach. If an average deposition of 14.5 cm  
743 at the embryo dune is assumed, the total amount of sediment deposited during  
744 this particular event was of  $905.7 \text{ kg m}^{-1}$  length of shoreline ( $0.43 \text{ m}^3 \text{ m}^{-1}$ ). Note  
745 that this does not consider sediment deposited at the dune toe and beyond  
746 because of the absence of instrumentation.

747

#### 748 7.4. Sediment input predicted over a storm event

749 Fig. 10E–G displays the analytical procedure output at an hourly scale.  
750 Prediction of sediment output from the beach based on wind speed and direction  
751 only resulted in a peak of transport rates coinciding with the peak of strong  
752 onshore winds (Fig. 10E), over-predicting the amount delivered to the dune  
753 ( $Q_n$  for this event =  $9470 \text{ kg m}^{-1}$ ). The introduction of thresholds for moisture  
754 content ( $\mu < 10\%$ ) and beach width ( $W > 0 \text{ m}$ ) as necessary conditions for  
755 transport removed the majority of strong onshore winds (Fig. 10F), resulting in  
756 improved predictions ( $Q_{\text{filtering}} = 3720 \text{ kg m}^{-1}$ ). Predicted transport was  
757  $Q_{\text{PTP}} = 1698 \text{ kg m}^{-1}$  ( $0.65 \text{ m}^3 \text{ m}^{-1}$ ) after considering  $F_c$  or  $F_c\mu$  (Fig. 10G), which  
758 was slightly higher but on the same order of magnitude as the observed  
759 deposition over the storm, thus confirming the viability of the modelling approach.  
760

761 **8. Discussion**

762

763 The filtering improved calculations of sediment input to the foredunes by  
764 eliminating periods of time where transport was predicted based solely on wind  
765 speed and direction, but where no transport occurred because of the effect of  
766 one or more limiting factors. The improvement made by incorporating both the  
767 fetch effect and moisture was significant and suggests that further advances in  
768 modelling instantaneous relations between wind speed, fetch distances, moisture  
769 content and transport over a variety of situations will aid in refining predictions.  
770 The results of the analytical procedure suggest, however, several areas where  
771 the two modelling steps can be further refined. The thresholds used in the  
772 filtering step for this particular study were quite conservative with the result that  
773 the number of PTPs identified is much greater than the 27 transport events  
774 actually observed over the same time period by Delgado-Fernandez and  
775 Davidson-Arnott (2011). As shown in Fig. 11, all observed transport events were  
776 included within the set of predicted PTPs; i.e., no actual transport events were  
777 missed. However, there were a number of predicted PTPs where no transport  
778 was observed. In the majority of cases this occurred where winds were slightly  
779 above the threshold for dry sand but transport did not occur because of moderate  
780 levels of moisture on the beach. Transport would have occurred with either  
781 stronger winds or drier sediments. In some cases transport may have been  
782 inhibited by factors which could not be measured by the remote station at  
783 Greenwich (e.g. topographic changes). In any case the filtering did not eliminate

784 observed transport events from the calculations suggesting appropriate threshold  
785 values at this site (i.e., no loss of data). Transport within a number of PTPs was  
786 also over-predicted. In many cases this was the result of the inadequacies of the  
787 modelling of transport rates associated with moderate wind speeds and  
788 moderate levels of surface moisture content and/or spatially complex patterns of  
789 moisture content. For example, during the first quarter of the storm described  
790 in Fig. 10, low wind speeds of  $\approx 10 \text{ m s}^{-1}$  yielded a short  $F_c$  of  $\approx 15\text{--}20 \text{ m}$ .  
791 Moisture ranged from 2 to 4% due to intermittent rain and  
792 thus  $F_{c\mu} = F_c$ .  $F$  oscillated from 30 to 50 m due to a relatively wide beach and  
793 oblique angle of wind approach. Because  $F_c < F$  transport was predicted with the  
794 same magnitude as the rate solely based on wind speed and direction (compare  
795 E and F in Fig. 10). The effect of both moisture and fetch was more visible during  
796 the second quarter of the storm, when strong wind speeds and larger moisture  
797 contents resulted in  $F_{c\mu} > F$ . This research will thus benefit from detailed studies  
798 on the combined effect of fetch distances and moisture content at the beach,  
799 because they play an important role in modifying the magnitude of calculated  
800 transport for individual PTPs.

801 The substantial differences in observed deposition with different techniques  
802 introduce uncertainty with respect to the appropriate ('true') value used in the  
803 comparison with predicted quantities. In part this reflects inadequacies in the  
804 number and placement of both bedframe stations and ED pins, and in particular  
805 a failure to recognise the ease with which a large number of ED pins could have  
806 been deployed. The simplicity and higher temporal resolution provided by placing

807 the ED pins in the field of view of the cameras greatly enhances the potential of  
808 the camera monitoring system for future studies of beach/dune interaction and  
809 changing dune morphology. The hourly time series of the ED pins permitted  
810 much better assessment of periods of erosion as well as accretion and indicated  
811 that net changes measured by sampling at relatively long time intervals (e.g., bi-  
812 monthly bedframe measurements) underestimate the gross amount of sand  
813 delivered to the dune. All ED pins recorded several periods of sand removal due  
814 both to wave and wind erosion (as observed from the cameras). This suggests  
815 that some of the sediment delivered from the beach to the embryo dune was  
816 never actually recorded by low temporal resolution techniques, because these  
817 integrated erosion and sand removal within net deposition observations.  
818 Nevertheless, they also serve to highlight the difficulty of distinguishing wave  
819 erosion and deposition from wind erosion and deposition in the area of  
820 overlapping influence, and the limitations associated with a few point  
821 measurements within this zone.

822 Efforts to fully explore the capabilities of the time series stored in the PEI GDB  
823 are currently being developed. The PEI GDB contains raster datasets and  
824 feature series with information about shoreline configuration, vegetation patterns,  
825 or spatial changes on moisture every hour. In particular, it is at the PTP level that  
826 the complexities associated with these factors may improve the model  
827 performance, especially during scenarios such as PTPs type C. However, in the  
828 broader context of sand transport prediction at the meso scale, two important  
829 aspects are worthy of consideration: 1) the potential benefits of adopting

830 probabilistic approaches versus a deterministic procedure; and 2) the potential  
831 for extracting estimates of key controlling variables, such as surface moisture  
832 content and beach width, from data measured at standard meteorological  
833 stations for the majority of situations where there is no direct monitoring of the  
834 beach and dune system. Probabilistic approaches are common in weather  
835 forecasting and estimate the probability of an event occurrence/magnitude based  
836 on past (historical) data whilst including information on the uncertainty of the  
837 prediction. However, they need historical records of several environmental  
838 factors and there is a lack of long-term datasets on sediment transport processes  
839 at the beach. The monitoring station at Greenwich has been collecting data for  
840 over a period of 2 years so further analysis of wind, supply limiting factors, and  
841 transport processes may provide a good basis for a probabilistic model.

842 Secondly, it would be worth exploring ways in which limiting factors such as  
843 beach surface moisture, snow and ice and beach width could be estimated from,  
844 e.g., hourly values for rainfall or snowfall, temperature, tidal range, average  
845 beach width and some simple storm surge and run-up model.

846 Finally, it is worth stressing that the purpose of this work was not to provide an  
847 absolute accurate prediction of sediment input to Greenwich Dunes over  
848 9 months (if this is possible at all) but to test the effectiveness of a modelling  
849 approach that explicitly acknowledges the key role played by supply-limiting  
850 factors such as moisture, fetch and vegetation in determining the actual sediment  
851 supply from the beach to coastal foredunes over periods of months and years.

852 The results demonstrate that an approach based on transport-limited models is

853 inadequate at this temporal scale and that improved accuracy in prediction will  
854 come not from small refinements to traditional transport-limited models, but  
855 rather from the incorporation of the supply-limiting complexities. Whilst some of  
856 the variables identified at Greenwich may be irrelevant at other sites (e.g., snow-  
857 ice cover), the thresholds associated with beach inundation or moisture content  
858 are probably more universal and others, such as pebble lag development and  
859 flotsam, may also be relevant. New time series based on the type of monitoring  
860 system deployed here are, thus, desirable as they will aid in identifying particular  
861 key factors regulating the frequency and magnitude of aeolian transport events at  
862 other beach–dune systems and provide a rich data base which can be used to  
863 generate an improved supply-limited approach to meso-scale modelling of  
864 sediment supply from the beach.

865

## 866 **9. Conclusions**

867

868 The analyses presented in this paper show the potential for improved predictions  
869 of sediment input to coastal dunes using a simple modelling approach  
870 incorporating two steps. The first step reduces prediction of sediment supply to  
871 the foredune by removing wind events that do not result in transport because of a  
872 high threshold for sediment movement due to the magnitude of one or more  
873 supply-limiting variables, and thus isolates periods of time (PTPs) where  
874 predictive efforts should focus. The second step introduces the effect of fetch  
875 distances and limiting factors such as surface moisture content, which regulate



876 the supply of sediment from the surface and thus reduce the magnitude of  
877 transport compared to that predicted by transport-limited models. The use of the  
878 modelling approach greatly improves calculations of sediment supply toward the  
879 dune area, and suggests that further improvements can be made through the use  
880 of similar monitoring systems in other coastal dune environments. Finally the  
881 results of this study show that further improvements in our ability to predict  
882 sediment supply to coastal foredunes will require improvements in our ability to  
883 measure sand transport from the beach and deposition in the foredune at the  
884 same temporal scale.

885

## 886 **Acknowledgements**

887

888 I would like to express special gratitude to the extensive reviews and major  
889 contributions by Robin Davidson-Arnott, who has provided many of the  
890 conceptual and methodological tools for this project. I would also like to thank the  
891 extensive feedback provided by Bernie Bauer, and his valuable ideas associated  
892 with the modelling. Together these two researchers have provided the core ideas  
893 of the work presented here. Bill Nickling and Ray Kostaschuck provided detailed  
894 comments over earlier drafts that have greatly improved the present manuscript.  
895 Special thanks are extended all the staff at Greenwich Dunes, especially Kirby  
896 Tulk, Allan Doyle, Tarah McFee, Roger Steadman, and Miguel Santos. This  
897 study was supported by a research grant from Prince Edward Island National  
898 Park and a Natural Sciences and Engineering Research Council of Canada

899 Discovery Grant to R. Davidson-Arnott, and by an Ontario Graduate Scholarship  
900 (Ministry of Training, Canada) to I. Delgado-Fernandez. Finally, I would like to  
901 thank Chris Hugenholtz and an anonymous reviewer, whose recommendations  
902 have greatly improved the final version of this paper.

903

#### 904 **References**

905

906 Bagnold, R.A., 1941. The physics of blown sand and desert dunes. London,  
907 Methuen, 265 pp.

908 Bauer, B.O. and Davidson-Arnott, R.G.D., 2003. A general framework for  
909 modelling sediment supply to coastal dunes including wind angle, beach  
910 geometry and fetch effects. *Geomorphology*, 49, 89-108.

911 Bauer, B.O. and Sherman, D.J., 1999. Coastal dune dynamics: Problems and  
912 Prospects. In: A.S. Goudie, I. Livingstone and S. Stokes (Editors), *Aeolian  
913 Environments, Sediments and Landforms*. John Wiley and Sons, pp. 71-  
914 104.

915 Bauer, B.O., Davidson-Arnott, R.G.D., Hesp, P.A., Namikas, S.L., Ollerhead, J.,  
916 Walker, I.J., 2009. Aeolian sediment transport on a beach: Surface  
917 moisture, wind fetch, and mean transport. *Geomorphology*, 105, 106-116

918 Belly, P., 1964. Sand movement by wind, U.S. Army Corps of Engineers CERC,  
919 Tech. Memo 1, 38.

920 Carson, M. A. and MacLean, P. A., 1986. Development of hybrid aeolian dunes:  
921 the William River dune field, northwest Saskatchewan, Canada. Canadian  
922 Journal of Earth Sciences, 23: 1974-1990

923 Chapman, D.M., 1990. Aeolian sand transport - an optimized model. Earth  
924 Surface Processes and Landforms, 751-760.

925 Christiansen, M.B. and Davidson-Arnott, R.G.D., 2004. Rates for landward sand  
926 transport over the foredune at Skallingen, Denmark and the role of dune  
927 ramps. Geografisk Tidsskrift, Danish Journal of Geography, 104(1): 27-36.

928 Coates, D. R. and Vitek, J.D., 1980. Thresholds in Geomorphology. Binghamton  
929 Symposia in Geomorphology International Series. Allen and Unwin,  
930 Boston, xii, 498 p.:

931 Darke, I., Davidson-Arnott, R.G.D. and Ollerhead, J., 2009. Measurement of  
932 beach surface moisture using surface brightness. Journal of Coastal  
933 Research, 25, 248-256.

934 Davidson-Arnott, R.G.D. and Law, M.N., 1990. Seasonal patterns and controls  
935 on sediment supply to coastal foredunes, Long Point, Lake Erie. In: K.F.  
936 Nordstrom, N.P. Psuty and R.W.G. Carter (Editors), Coastal Dunes:  
937 Form and Process. John Wiley & Sons, pp. 177-20.

938 Davidson-Arnott, R.G.D. and Law, M.N., 1996. Measurement and prediction of  
939 long-term sediment supply to coastal foredunes. Journal of Coastal  
940 Research, 12 pp. 654-663.

941 Davidson-Arnott, R.G.D., Yang, Y., Ollerhead, J., Hesp, P.A. and Walker, I.J.,  
942 2008. The effects of surface moisture on aeolian sediment transport

943 threshold and mass flux on a beach. *Earth Surface Processes and*  
944 *Landforms*, 33, 55 – 74.

945 Davidson-Arnott, R.G.D. and Bauer, B.O., 2009. Aeolian sediment transport on a  
946 beach: Thresholds, intermittency, and high frequency variability.  
947 *Geomorphology*. 105, 117-126

948 Delgado-Fernandez, I., Davidson-Arnott, R.G.D. and Ollerhead, J., 2009.  
949 Application of a remote sensing technique to the study of coastal dunes.  
950 *Journal of Coastal Research*, 25 (5), 1160-1167.

951 Dong, Z., Wang, H., Liu, X. and Wang, X., 2004. The blown sand flux over a  
952 sandy surface: a wind tunnel investigation on the fetch effect.  
953 *Geomorphology*, 57, 117-127.

954 Fryberger, S.G. and Dean, G., 1979. Dune forms and wind regime. In: E.D.  
955 McKee (Editor), *Global Sand Seas*, pp. 141-151.

956 Fryrear, D. W., Bilbro, J. D., Saleh, A., Schomberg, H., Stout, J. E., and Zobeck,  
957 T. M., 2000. RWEQ: Improved Wind Erosion Technology. *J. Soil Water*  
958 *Conserv.* 55, p. 183

959 Gillette, D.A., Herbert, G., Stockton, P.H. and Owen, P.R., 1996. Causes of the  
960 fetch effect in wind erosion, *Earth Surf. Proc. Land.* 21, 641-659.

961 Hesp, P.A., 1988a. Morphology, dynamics and internal stratification of some  
962 established foredunes in southeast Australia. *Journal of Sedimentary*  
963 *Geology*, 55, pp. 17-41.

964 Hesp, P.A., 1988b. Surfzone, beach and foredune interaction on the Australian  
965 southeast coast. *Journal of Coastal Research*, 3, 15-25.

966 Hesp, P. A., 2002. Foredunes and blowouts: initiation, geomorphology and  
967 dynamics. *Geomorphology*, 48, 245–268.

968 Hesp, P.A., Davidson-Arnott, R.G.D., Walker, I.J. and Ollerhead, J., 2005. Flow  
969 dynamics over a foredune at Prince Edward Island, Canada.  
970 *Geomorphology*, 65, 71-84.

971 Hotta, S., Kubota, S., Katori, S. and Horikawa, K., 1984. Sand transport by wind  
972 on a wet sand surface. *Proceedings of the 19th Coastal Engineering  
973 Conference, ASCE, New York*, pp. 1265-1281.

974 Hsu, 1974. Computing eolian sand transport from routine weather data.  
975 *Proceedings of the 14<sup>th</sup> Conference on Coastal Engineering, ASCE, New  
976 York*, 1619-1626.

977 Hunter, R.E., Richmond, B.M., Alpha, T.R., 1983. Storm-controlled oblique dunes  
978 of the Oregon coast. *Geological Society of America Bulletin*, 94, 1450-  
979 1465

980 Jackson, N.L. and Nordstrom, K.F., 1997. Effects of time-dependent moisture  
981 content of surface sediments on aeolian transport rates across a beach,  
982 Wildwood, New Jersey. *U.S.A. Earth Surface Processes and  
983 Landforms*, 22: 611-621.

984 Kadib, A.L., 1964. Calculation procedure for sand transport by wind on natural  
985 beaches, *Miscellaneous paper 2, 64, US Army Coastal Engineering  
986 Research Center*.

987 Kroon, A. and Hoekstra, P., 1990. Eolian sediment transport on a natural beach.  
988 *Journal of Coastal Research*, 367-380.

- 989 Law, M. N., 1989. Sand Transport from Beaches to Coastal Dunes. M.Sc.  
990 Thesis, University of Guelph, 173 pp.
- 991 Lettau K. and Lettau, H., 1977. Exploring the World's Driest Climate. University of  
992 Wisconsin-Madison, IES Report 101, 110-147.
- 993 Logie, M., 1982. Influence of roughness elements and soil moisture on the  
994 resistance of sand to wind erosion. In: D.H. Yaalon (Editor), Aridic soils  
995 and geomorphic processes. Catena Supplement 1, Braunschweig, 161-  
996 173.
- 997 McKenna Neuman C, Muljaars Scott M. 1998. A wind tunnel study of the  
998 influence of pore water on aeolian sediment transport. Journal of Arid  
999 Environments 39, 403–419.
- 1000 McKenna Neuman, C. and Nickling, W.G., 1989. A theoretical and wind tunnel  
1001 investigation of the effects of capillary water on the entrainment of  
1002 sediment by wind. Canadian Journal of Soil Science, pp. 79-96.
- 1003 Namikas, S.L. and Sherman, D.J., 1995. A review of the effects of surface  
1004 moisture content on aeolian sand transport. In: V.P. Tchakerian (Ed.),  
1005 Desert Aeolian Processes. Chapman and Hall Ltd., London, 269-293.
- 1006 Nickling, W.G. and Davidson-Arnott, R.G.D., 1990. Aeolian sediment transport on  
1007 beaches and coastal sand dunes. In: Davidson-Arnott, R.G.D. (Ed.),  
1008 Proceedings of the Symposium on Coastal Sand Dunes, National  
1009 Research Council of Canada, 1-35.

1010 Nordstrom, K. F. and Jackson, N. L., 1993. The role of wind direction in eolian  
1011 transport on a narrow sand beach. *Earth Surface Processes and*  
1012 *Landforms*, 18, 675-685.

1013 Ollerhead, J., Johnson, P., Davidson-Arnott, R. G. D., Walker, I., and Hesp, P.  
1014 A., 2003. Sediment supply to coastal foredunes, Greenwich Dunes.  
1015 *Proceedings Canadian Coastal Conference, CCSEA*, pp. 12.

1016 Psuty, N.P., 1988a. Sediment budget and dune/beach interaction. *Journal of*  
1017 *Coastal Research, Special Issue 3*, pp. 1–4.

1018 Pusty, N.P. (Ed.), 1988b. Dune/Beach interaction. *Journal of Coastal Research,*  
1019 *Special Issue No. 3*, 136 pp.

1020 Ruz, M.H. and Meur-Ferec, C., 2004. Influence of high water levels on aeolian  
1021 sand transport: upper beach/dune evolution on a macrotidal coast,  
1022 *Wissant Bay, northern France. Geomorphology*, 60, 73-87.

1023 Sarre, R.D., 1987. Aeolian sand transport, *Progress in Physical Geography*, 157-  
1024 182.

1025 Sarre, R.D., 1989. Aeolian sand drift from the intertidal zone on a temperate  
1026 beach: potential and actual rates. *Earth Surface Processes and*  
1027 *Landforms*, 247-258.

1028 Sherman, D.J. and Bauer, B.O., 1993. Dynamics of beach-dune systems.  
1029 *Progress in Physical Geography*, 413-447.

1030 Sherman, D.J. and Hotta, S., 1990. Aeolian sediment transport: theory and  
1031 measurement. In: K.F. Nordstrom, N.P. Psuty and R.W.G. Carter

1032 (Editors), Coastal Dunes: Process and Morphology. John Wiley and Sons,  
1033 New York, pp. 17-37.

1034 Short, A.D. and Hesp, P.A., 1982. Wave, beach and dune interactions in  
1035 southeast Australia. *Marine Geology*, 48, 259-284.

1036 Spies, P.J. and McEwan, I.K., 2000. Equilibration of saltation. *Earth Surface*  
1037 *processes and Landforms*, pp. 437-453.

1038 Stout, J.E. 1990. Wind erosion within a simple field. *T. ASAE* 33, 1597-1600.

1039 Wahid, A.H., 2008. GIS-Based modelling of wind-transported sand on the Qaa  
1040 Plain Beach, Southwestern Sinai, Egypt. *Journal of Coastal Research*, 24  
1041 (4), pp. 936-943.

1042 Walker, I.J., Hesp, P.A., Davidson-Arnott, R.G.D. and Ollerhead, J., 2003.  
1043 Topographic effects on airflow over a vegetated foredune: Greenwich  
1044 Dunes, Prince Edward Island, Canada. *Proceedings Coastal Sediments*  
1045 '03. ASCE, New York, pp. 15.

1046 Walker, I. J., Hesp, P.A., Davidson-Arnott, R.G.D., and Ollerhead, J., 2006.  
1047 Topographic Steering of Alongshore Airflow over a Vegetated Foredune:  
1048 Greenwich Dunes, Prince Edward Island, Canada. *Journal of Coastal*  
1049 *Research*, 22, 1278-1291.

1050 Wiggs, G.F.S., Atherton, R.J. and Baird, A.J., 2004a. Thresholds of aeolian sand  
1051 transport: establishing suitable values. *Sedimentology*, 51, 95-108.

1052 Wiggs, G.F.S., Baird, A.J. and Atherton, R.J., 2004b. The dynamic effects of  
1053 moisture on the entrainment and transport of sand by wind.  
1054 *Geomorphology*, pp. 13-30.



1055 Wolman, M.G. & W.P Miller. 1960. Magnitude and frequency of forces in  
1056 geomorphic processes. *Journal of Geology*, 68, 54-74.

1057 Yang, Y. and Davidson-Arnott, R.G.D., 2005. Rapid Measurement of Surface  
1058 Moisture Content on a Beach. *Journal of Coastal Research*, 21, 447-452.

1059

1060 **List of Figures**

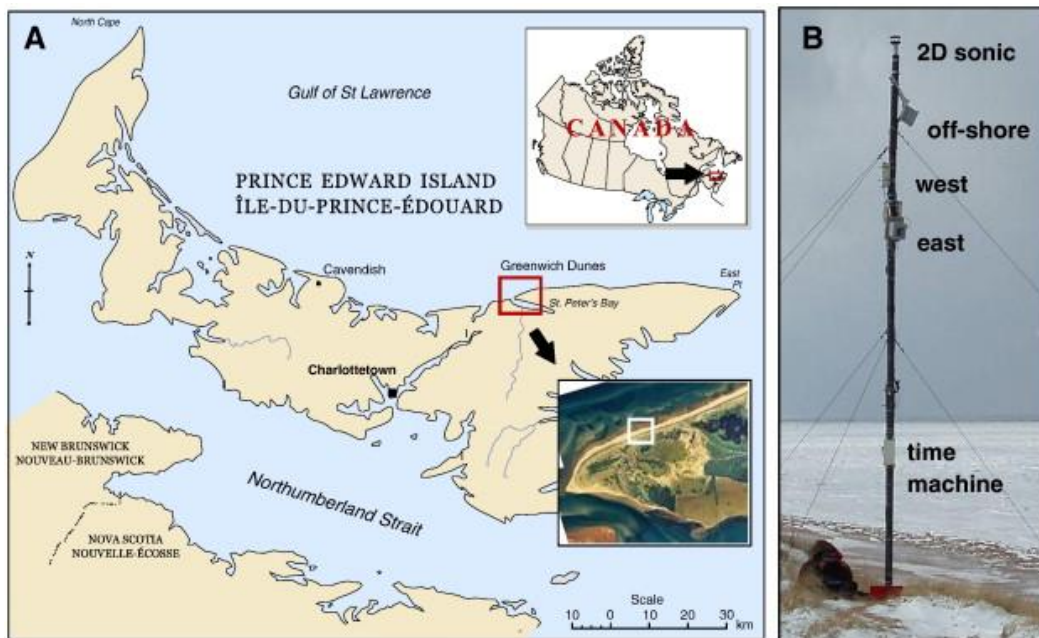


Fig. 1. A) Location of study area; B) Principal components of the camera system and 2-Dimensional Windsonic anemometer located on top of the 6 m mast (elevation over the beach surface of approximately 14 m).

1061

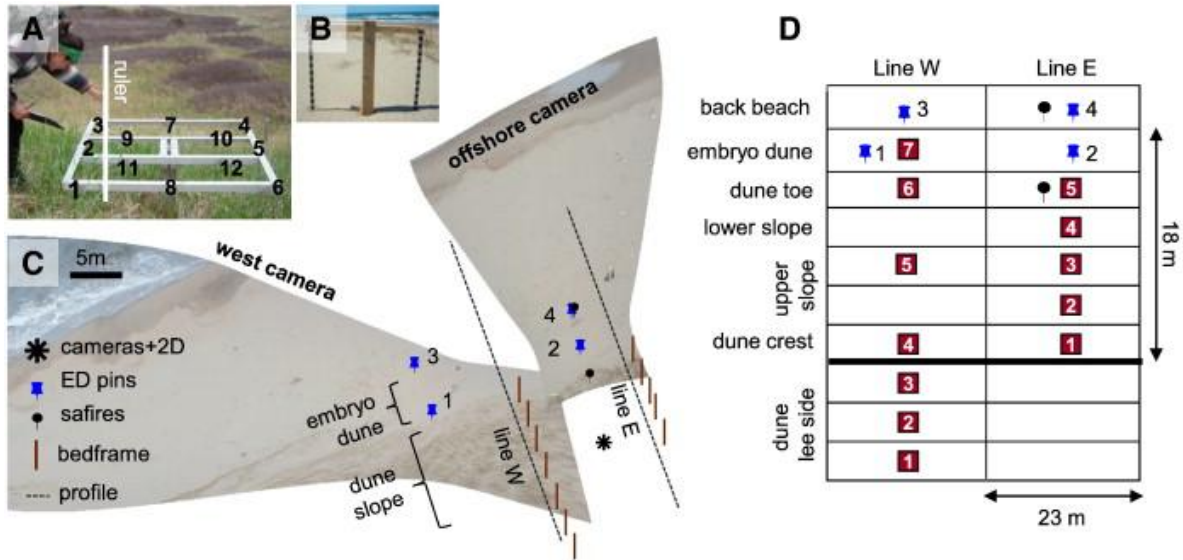


Fig. 2. A) Bedframe device deployed at a bedframe post at the dune. The average of the distance from the ground to the 12 points marked in the image provides data on surface elevation change at that location (Ollerhead et al., 2003). B) Erosion-deposition (ED) pin; C) Location of transport measurement points and survey profiles with respect to the camera system; D) Distribution of bedframe posts along line E and W, covering a total area of 46 m alongshore x 18 m across the dune. Each bedframe post represented an area of 23 m alongshore x 3 m cross-shore. No bedframe posts were located on line E beyond the dune crest. Bedframe posts 1–3 in line W were used for monitoring but not in actual calculations (Section 7.1). Safires and ED pins are included in the closest grid cell. Topographic details of lines E and W are included in Fig. 8.

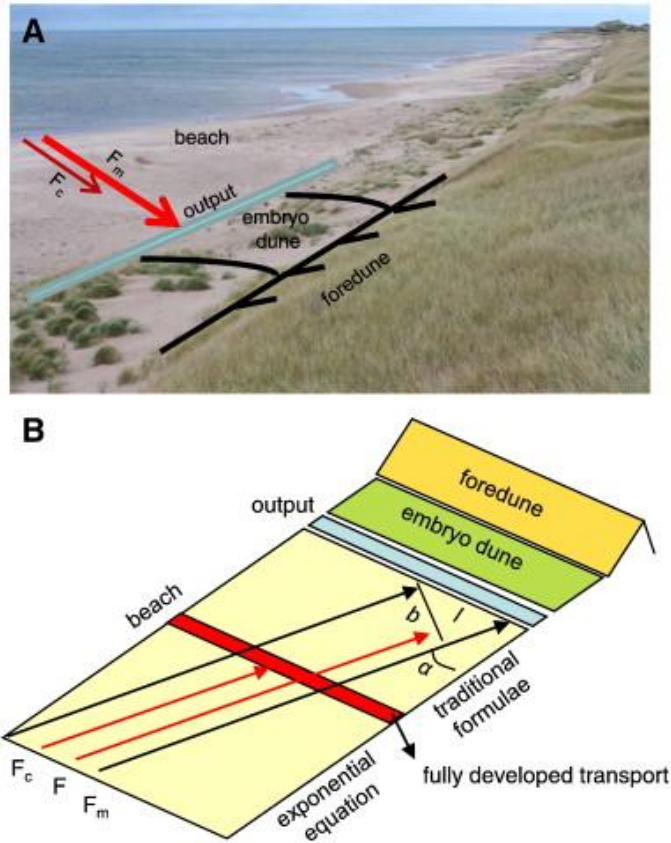


Fig. 3. Framework for modelling aeolian sediment output from the beach to the dune based on the study by Bauer and Davidson-Arnott (2003). A) Image taken by the east-facing camera at Greenwich, showing the location of the output area; B) Scheme for modelling. The red line on the beach surface indicates the area where transport is fully developed for an incoming wind speed.  $F_m$  is the maximum available fetch,  $F_c$  is the critical fetch and  $\alpha$  is the angle of wind approach. Traditional formulae to predict sediment transport rates may be applied where  $F > F_c$ , whilst transport follows an exponential relation with distance where  $F < F_c$ .

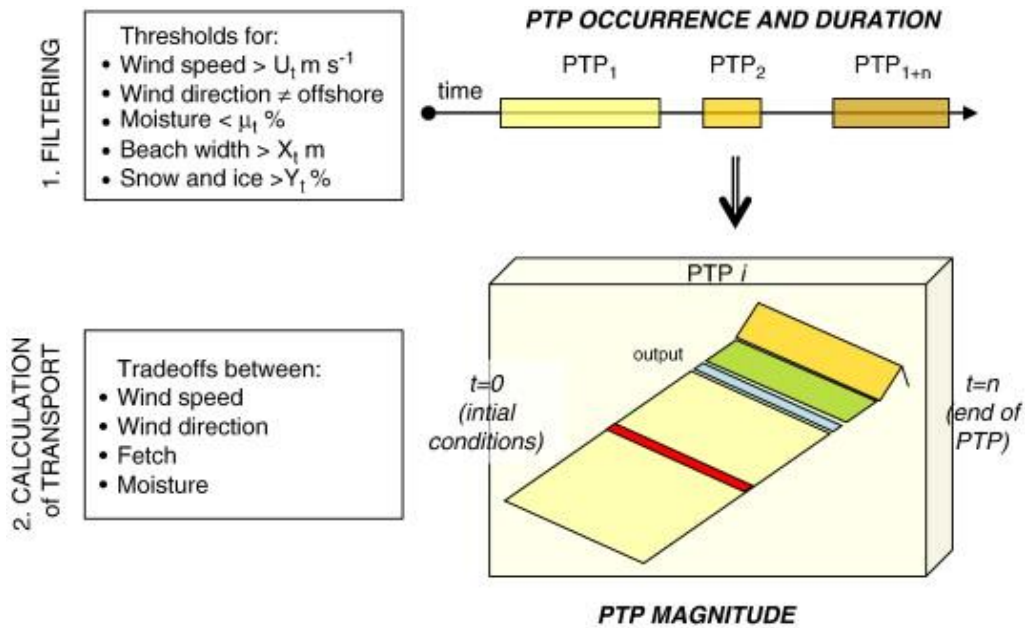


Fig. 4. Modelling approach following two steps: 1) the filtering reduces the time series and isolates potential transport periods (PTPs) providing valuable information about potential occurrence and duration of transport events and 2) calculation of transport focuses on particular PTPs, where the magnitude of sediment input to the foredunes is computed considering the fetch and the cosine effects and moisture content. This step may allow incorporation of the spatial variability of key factors, such as variations of beach width and moisture content over a particular event.

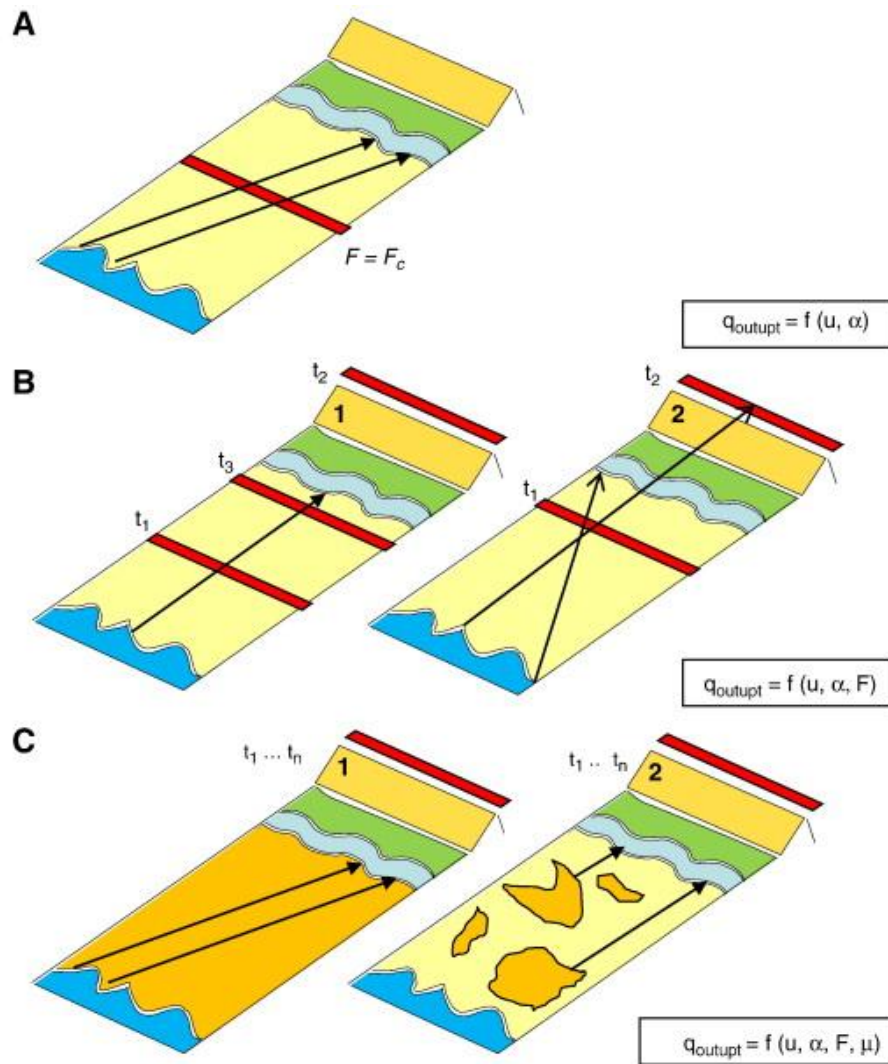


Fig. 5. Modelling scenarios for calculating sediment output from the beach ( $q_{output}$ ) and hypothetical examples of potential transport periods (PTPs). Note that a red band beyond the foredune crest indicates that the fetch distance is shorter than the critical fetch ( $F < F_c$ ) at the output area and thus the fetch effect needs to be considered. A) Type A PTP: transport at the output area is solely based on wind speed and direction and may be predicted using Bagnold-type equations (e.g., oblique-onshore winds over a dry surface); B) Type B PTPs: the fetch effect needs to be considered during  $t_2$  periods. The beach surface is dry

but the area (red line) where  $F = F_c$  changes spatially because of increases on wind speed (B1) or changes in the angle of wind approach (B2). B1 shows an example of a situation with a low wind speed ( $t_1$ ) becoming increasingly strong ( $t_2$  — longer  $F_c$ ), followed by a final period of low wind speed ( $t_3$ ). B2 shows an example of a strong oblique wind ( $t_1$ ) shifting to directly onshore ( $t_2$  —  $F_c$  remains constant but  $F$  decreases during onshore winds). C) Type C PTPs: both the fetch effect and moisture (in orange) need to be considered. Uniform moisture (C1) increases the  $F_c$  and thus transport may never fully develop at the beach. Moisture patches (C2) reduce the available  $F$  between the onset of transport and the output area.

1065

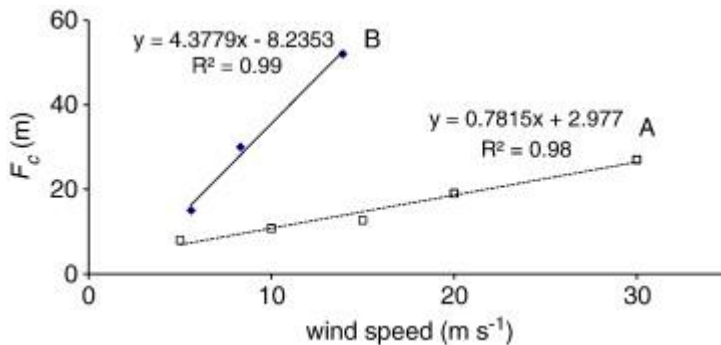


Fig. 6. Correlation between wind speed and critical fetch ( $F_c$ ) for the data presented by A) Spies and McEwan (2000) and B) Davidson-Arnott and Law (1996). Note that wind speed ( $U$ ) for curve A has been calculated from friction velocities ( $u^*$ ) reported by Spies and McEwan using the Law of the Wall ( $U = \ln(z/z_0) u^*/k$ ) and assuming a grain size of 0.25 mm.

1066

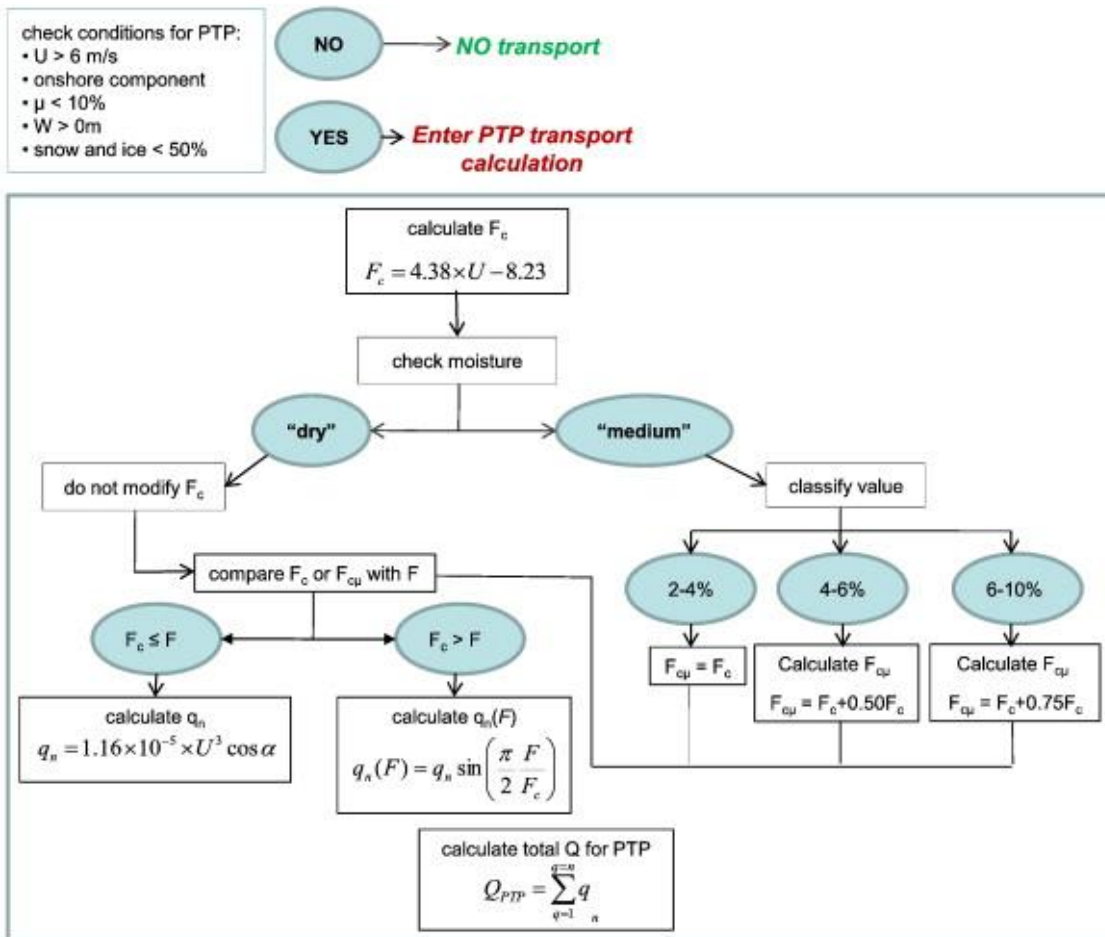


Fig. 7. Modelling steps and analytical procedure applied to hourly records of wind speed ( $U$ ) and direction ( $\alpha$ ), fetch distance ( $F$ ), critical fetch distance ( $F_c$ ) and moisture ( $\mu$ ) for potential transport periods (PTPs) isolated by the filtering.

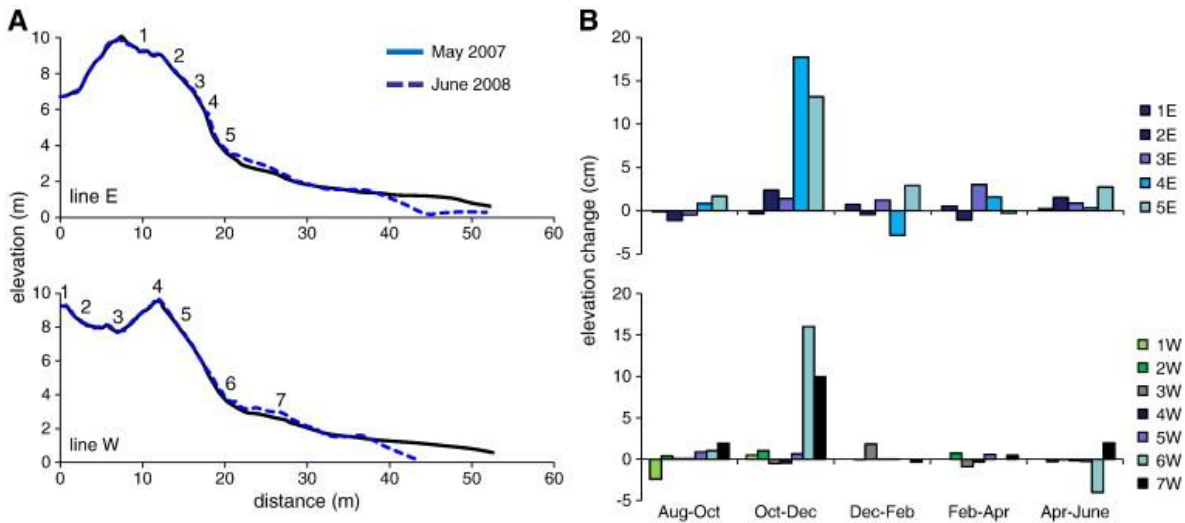


Fig. 8. A) Topographic profiles on May 2007 and June 2008. The numbers over the profiles show the location of bedframe posts; B) Bi-monthly net changes from August 2007 to June 2008 detected with the bedframe technique. Note that the largest change on the foredune stoss slope is of + 3 cm in post 3E. Most significant changes occurred from October to December 2007 at the lower sections of the dune (posts 4–5E and 6–7 W).

1068

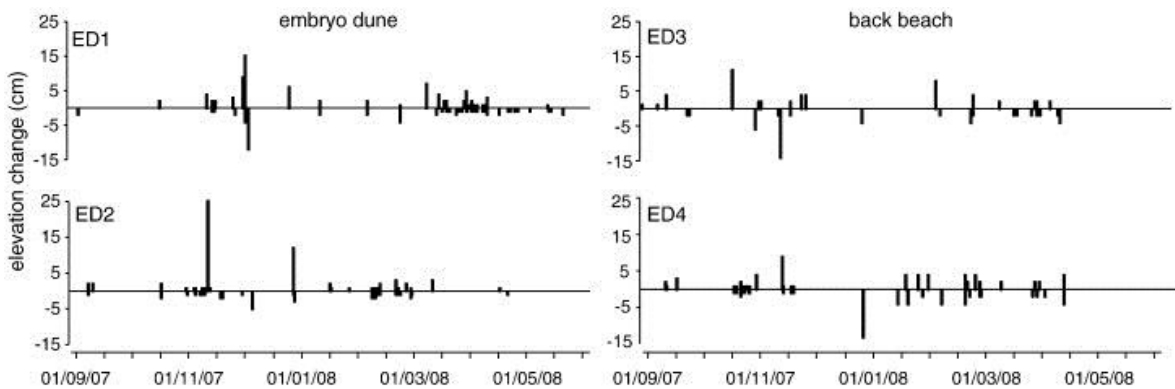


Fig. 9. Erosion-deposition (ED) pin records show several periods of accumulation and erosion. The majority of changes are of less than  $\pm 5$  cm, but there are several hourly changes of  $\pm 15$  cm and a single record of + 25 cm associated with the in



November 9, 2007 (Section 7.3).

1069

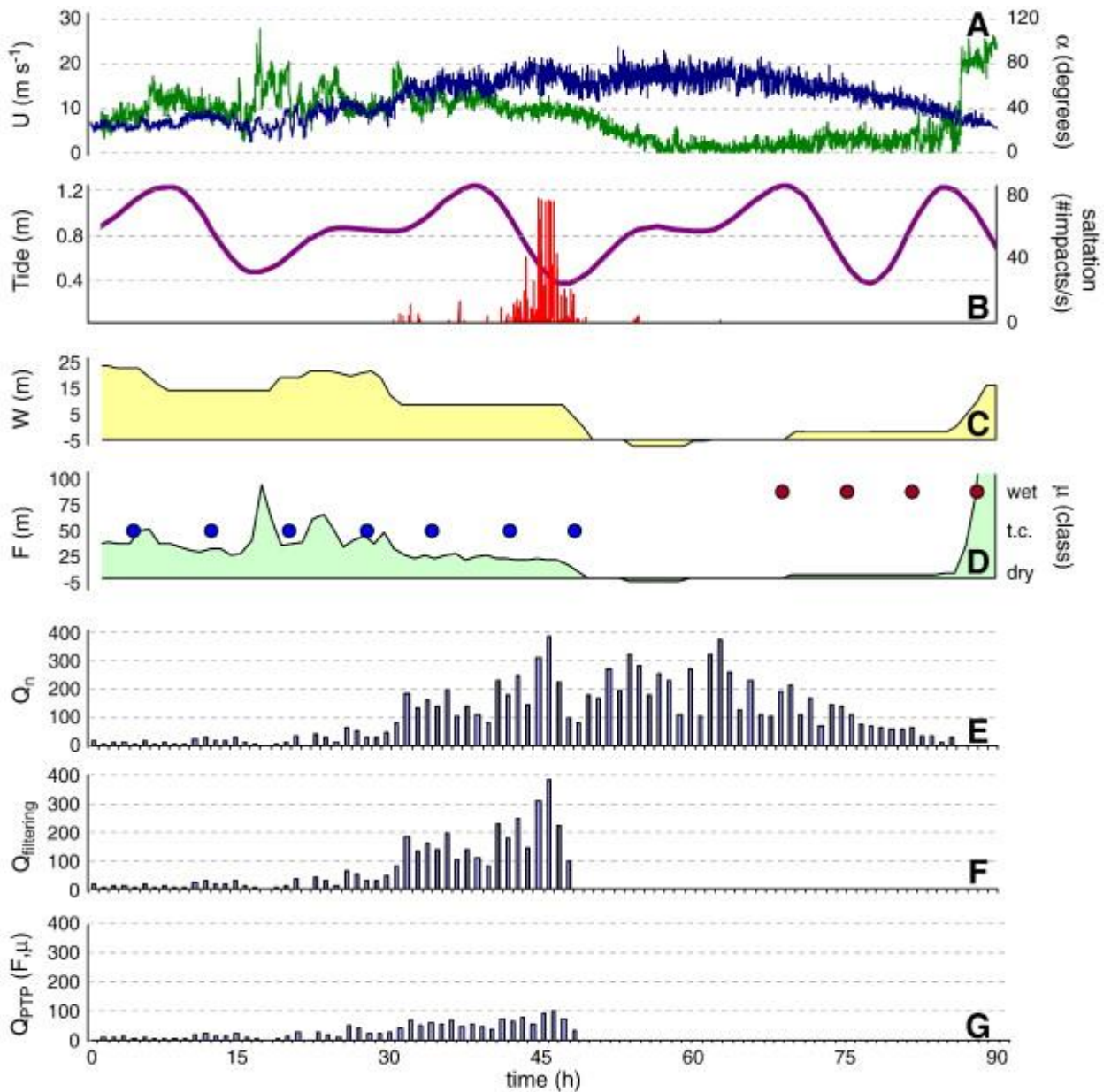


Fig. 10. Modelling output for a 90-hours storm approaching Greenwich from the North on November 9, 2007. A) 2-min records of wind speed ( $U$ ) and direction ( $\alpha$ ); B) saltation intensity and tide elevation; C) beach width ( $W$ ); D) fetch distance ( $F$ ) determined by beach width and wind direction, and classified moisture values ( $\mu$ ); E) hourly transport

based on wind speed and direction ( $Q_n$ ); F) output of the filtering step ( $Q_{\text{filtering}}$ ); G) output of the calculation of transport over the isolated potential transport periods ( $Q_{\text{PTP}}$ ) including fetch distance and moisture. Transport in E–F is expressed in  $\text{kg m}^{-1}$ .

1070

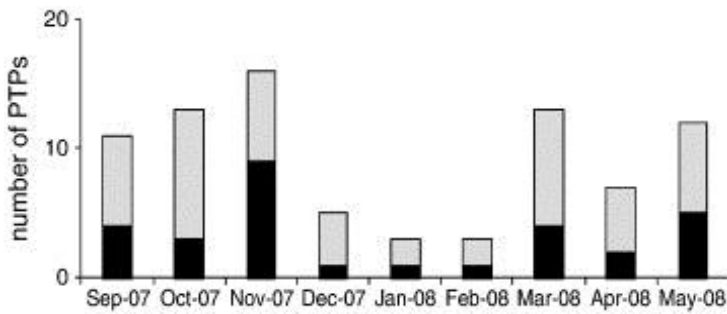


Fig. 11. Isolated potential transport periods (PTPs) where transport was observed (black) and where transport was not developed (grey).

1071